

PHSX 444: Lab 01; Magnetic Susceptibility

William Jardee

October 3, 2021

Introduction

An important characteristic to all materials is how they react to external magnetic fields. The strength of the response is quantified in a material's magnetic susceptibility, χ_m , which is dependent on a variety of internal factors. The scope of those factors is past this lab, so let's jump to the application of χ_m . As a magnetization is induced in the material from an external field, B

$$U_{potential} = -\frac{\chi_m B^2 V}{2\mu_0} \quad (1)$$

Where V is the volume of the material, and μ_0 is the magnetic constant. If a material is raised to a higher energy state in the presence of a B , then $\chi_m < 0$ and we call this a diamagnet. If the energy is lowered, then $\chi_m > 0$ and we call this a paramagnet. In a diamagnet, a magnetization is caused in the material anti-parallel the external magnetic field, and in a paramagnet the magnetization is parallel the external magnetic field.

There is a special type of paramagnet, called a ferromagnet. These are permanent magnets like a fridge magnet that seem to permanently hold a magnetization in them. Ferromagnets have a $\chi_m > 0$, but their internal magnetization doesn't change unless put into a very strong external magnetic field or are warmed up past their Currie Temperature, the temperature where their magnetization starts to break down. There are other, more exotic types of materials, like superconductors or antiferromagnets. But, they require more advanced setups than what we intend to use are required to analyze these materials.

Experimental Methods

We decided to measure χ_m using the Guoy Technique. The Guoy Technique uses a strong magnetic field between two vertical, parallel magnets to induce a field in a sample. This induced field then either repels or attracts the magnet apparatus. The strength of this interaction is measured by observing how much the weight of the apparatus changes, which is reported by a scale as a mass. A heavier weight means a push or a pull down, and a lighter weight means the opposite. In measuring how much this sample pulled or pushed above and below the center of the B-field produced by the magnets, the magnetic susceptibility, χ_m , of the sample can be measured. Below is a picture of a similar apparatus to what was used.

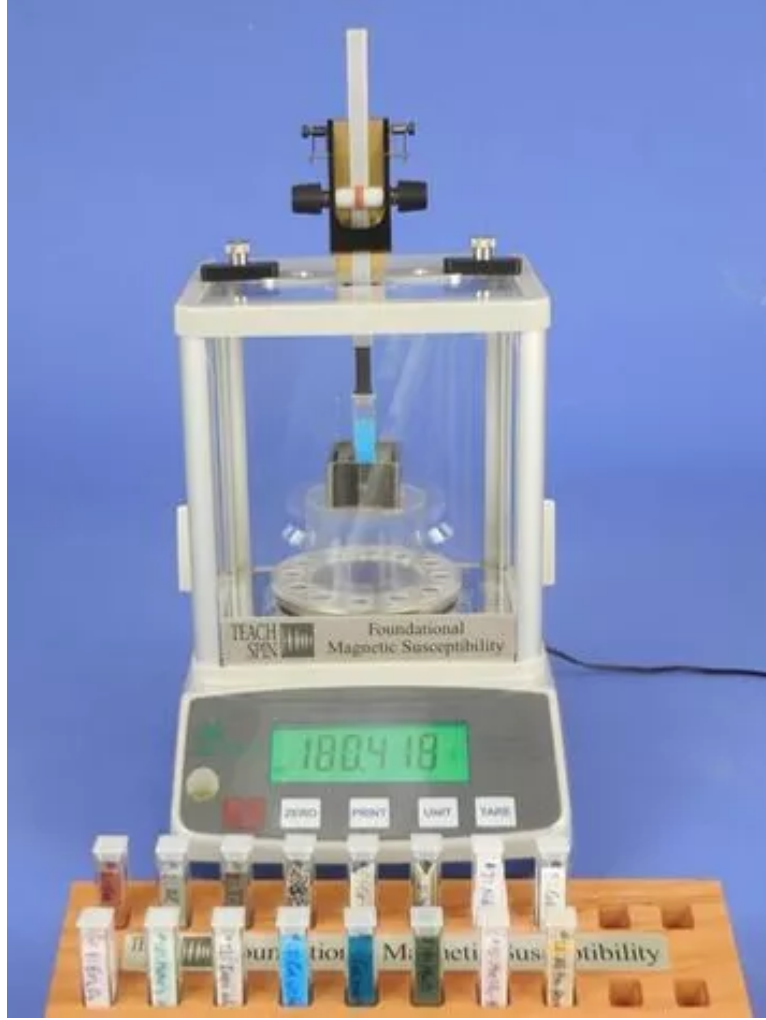


Figure 1: An illustration of the Guoy apparatus [6]

You can see a high precision scale (measured to an accuracy of 0.001 g) with a plastic stand holding two parallel permanent magnets. Being lowered from the mechanism on top of the scale is a sample, 16 of which were provided and will be expanded on in the Results and Analysis section.

In order to get data about the type of magnetism each sample holds, we will need to do three different measurements. We will refer to the first setup below in **figure 2** as the “far position”, the middle as the “high position”, and the left as the “low position”. In the derivation of the magnetic susceptibility, which can be seen in full in [1], a couple simplifying assumptions lead us to:

$$\Delta m = \frac{\chi_m A}{2\mu_0 g} (B_{top}^2 - B_{Bottom}^2) = \frac{\chi_m A}{2\mu_0 g} B_{center}^2 \quad (2)$$

The primary assumptions we have made were: 1. the B-field in the far position is negligible to the field from the two magnets at its strongest point. This was measured with the far position measurements and will be touched on in the Results and Analysis. 2. The

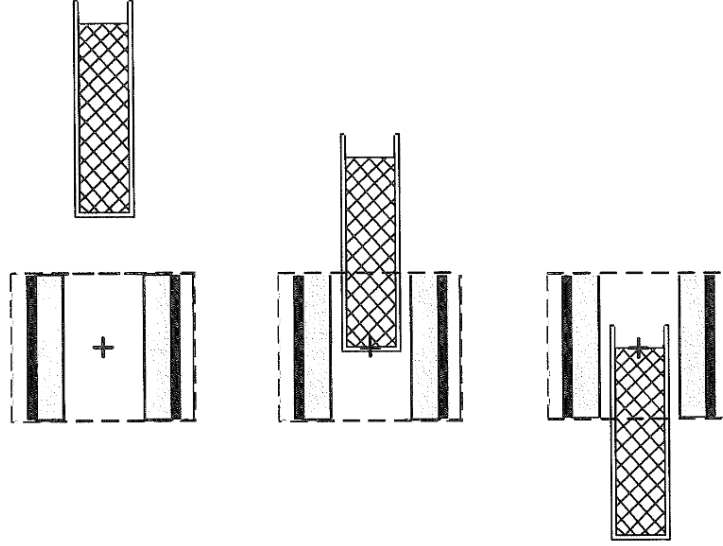


Figure 2: An illustration of the Guoy Technique [1]

sample is perpendicular to the horizontal and the component of forces not in the vertical direction are negligible. This allows all of the magnetic repulsion/attraction between the sample and the magnets to be estimated as the observed change in mass. This effect should be negligible since care can be taken to get the sample roughly parallel to the magnets.

The magnetic field between the two magnets in the apparatus was measured by inserting a copper loop into the center of the field and sending a current through it to induce a field. This current was ranged from 0.50 A to 0.90 A, taking measurements on a 0.05 A interval. To better understand the apparatus, the controlled B-field was placed with the bottom of the loop at the the high position and the low position. It was also arrange so that the loop's B-field was parallel the magnets' and perpendicular. As was expected, it was found that when the loop was in the high position and parallel the magnets' field was the only time the impact seemed measurable. In this position the gradient of the loop's B-field is least symmetrical in between the magnets and is in an orientation that interacts with the field. The data from this measurement can be seen in the Results and Analysis section, along with the calculated B-field and error.

Each of the provided samples Δm were measured at the far, high, and low positions. This allowed each's impact in the far position to be analyzed and to check our first assumption above; that the B-field on the far end of the sample is negligible. Since there was no exact measuring device in the scale box, there was no way to get a ruler into the scale box, and the low position went below where the high precision knob on the lowering device would let us go, each measurement had to be done by eyeballing the position. The far position and low positions were all taken at the highest and lowest heights the lowering mechanism would allow, so each was uniform in placement. There was a small circle in the center of the box that held the two magnets. We centered the bottom of the sample's curvette with that circle for each high position. While there may be error introduced through this method, all measurements were taken at the same height for each sample, so if any error trends were found, they would be systematic in nature and could be dealt with clever data analysis. Each

time a new sample was used, the mass of the plastic and magnet setup were measured. Doing this step meant any zero-point drift that happened inside the scale during the measurement session could be ignored by finding Δm from the most recent possible measurement point. These points could also be analyzed after the fact to look for any notable trends in the bias of the measurements, correcting for any that showed up.

Along with the 16 samples provide and requested to be analyzed, we provided two more that may provide some interesting insights. We chose Great Value brand Iodized Salt and Morton brand Himalayan Pink Salt. It was hypothesized that both these salts would have the same χ_m value.

To analyze the linearity of the magnetic susceptibility, a diamagnet (Copper), paramagnet (Aluminium), and a ferromagnet (Cobalt Wire) were measured at 21 different levels using a high precision knob on the lowering device provided with the apparatus. Each rotation of the knob supporting the height of the sample changed the height by 0.635 mm. We chose to do steps of 4 rotations, so each data point was 2.54 mm. The total displacement from the center was 25.4 mm up and 25.4 mm down.

Results and Analysis

Magnetic Field Calibration

Below are the measured masses at appropriate inputted currents (graph 3a). Doing a linear fit on the data gave us a slope of 3.96 ± 0.04 g/A. The length of the wire was 9.9 ± 0.1 mm. So, the relationship between the change in mass and B is:

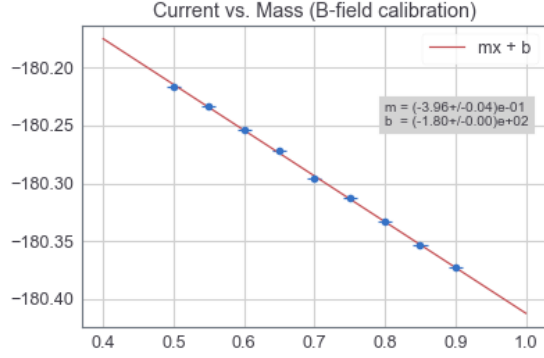
$$\Delta m = \frac{i(0.01)B}{g} \quad (3)$$

With i being the current given sent through the wire. Using a $g = 9.8026$ m/s² [2], $B = 0.389 \pm 0.004$ T. This fits well within the realm of what we expected, as the users manual for the lab said the strength should be about 0.4 T. It is common practice to check on the residuals to ensure that our fit was the correct choice. If the spread of the residuals looks randomly above and below the $y = 0$ line, then our fit is appropriate. As we can see from graph 3b, a linear fit seems an appropriate choice here.

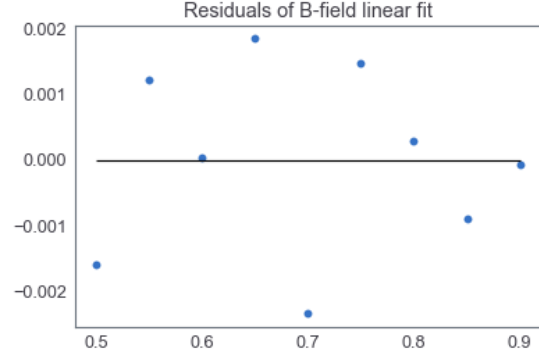
We measured the mass of the magnet and mount between every sample, and we can see in graph 4 that the wiggle in starting points seems random. This indicates that the dominating source of change of the starting position of the weights is based on an internal hysteresis, opposed to a general drift. These points are plotted according to the measurements taken in chronological order. The strong drop seen towards the end of the graph is the result of re-calibrating the data on the second day of measurements. We can see the importance of remeasuring our zero point before every sample, as it increased our accuracy by more than the error given by the manual would indicate.

Measuring Δm and χ_m

All the data collected can be seen in tables in Appendix A.



(a) current input in Amps along the x-axis, and read mass in grams along the y-axis. Error bars of 0.001 are given on the mass and 0.01 Amps on the current. A superimposed linear fit is given, with an equation $-0.00396x - 180$.



(b) The residuals of the line fit to the left.

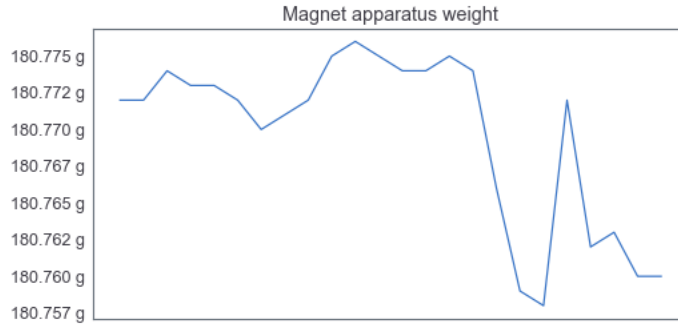


Figure 4: The initial weights before introducing each sample. The points are given in chronological order, with the first trial on the far left.

Analyzing our initial assumption that the Δm at the end of the sample farthest away, we measured each sample in the far position and plotted the effect in 5. The bounds are $\pm \frac{1}{4}$ the max Δm in the low position. The horizontal line is the average initial weight of the magnet apparatus between measurements. From this, we can see that the effect in the far position is negligible; thus, we are allowed to throw away the B_{top}^2 in 2.

Using 2 rewritten to

$$\chi_m = \Delta m \frac{2\mu_0 g}{AB^2} \quad (4)$$

Where A is now our cross-sectional area of 1 cm by 1 cm. In order to compare this value against values found online we translated them to molar χ_m

$$\chi_{molar} = \frac{W}{\rho} \quad (5)$$

Where W is the molar mass, and ρ is the density. To find the density, the masses were weighed individually right after the scale was calibrated and heights were measured by using

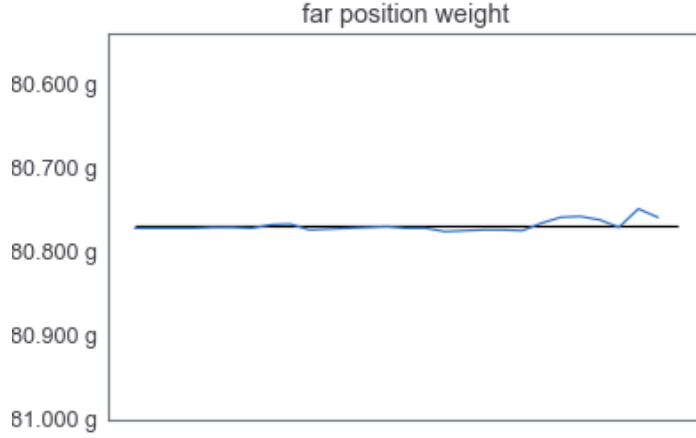


Figure 5: Measured mass in the far position. The points are given in chronological order, with the first trial on the far left.

a ruler to measure from the bottom of the sample to the top. For granular samples the top was determined to be the average surface level after being shaken till approximately level. All of these data points can be found in Appendix A. easily

Once the magnitude of χ_{molar} was found this way, they were assigned diamagnetic, paramagnetic, or ferromagnetic. As discussed earlier, diamagnets repel the external B_0 , so the Δm in the high position should be negative and Δm in the low position should be positive. The opposite is true for the paramagnet. Since we do not expect B_0 to be large enough to change the magnetization of any ferromagnets, it is expected that the ferromagnet's Δm will have the same sign in the high and low positions. Below is a table of all 18 samples, the 16 provided and the 2 brought in, and the online classification and our classification. Any cells that are empty were values that weren't found online.

Comparing the iodized salt and Himalayan pink salt, their χ_{molar} are very close to each other. However, the pink salt had 94% the density of the iodized salt but the same χ_{molar} . It seems that whatever characteristics gave the diamagnetic properties to the iodized salt were also produced in the Himalayan salt.

sample	name	ours	online	our χ_{molar} m ³ /mol	online χ_{molar}
1	copper	dia	dia	(-1.88+/-0.04)e-5	-5.460e-6
2	aluminum	para	para	(1.683+/-0.033)e-6	1.650e-5
3	titanium	para	para	(0.261+/-0.005)e-3	1.530e-4
4	bismuth	dia	dia	(-0.588+/-0.012)e-3	-2.800e-4
5	colbalt wire	para	ferro	(0.273+/-0.005)e-2	
6	pyrolytic graphite	dia		(-1.660+/-0.033)e-4	
7	neodymium choride	para	para	(0.680+/-0.013)e-2	
8	gadolinium oxide	ferro		(-0.423+/-0.008)e-2	5.320e-2
9	erbium oxide	ferro		(0.204+/-0.004)e-3	7.392e-2
10	mohrs salt	ferro		(-0.992+/-0.020)e-2	
11	irom alum	ferro	para	(-0.188+/-0.004)e-1	
12	blue vitriol	para		(0.231+/-0.005)e-2	1.330e-3
13	copper acetate	para		(0.933+/-0.018)e-3	
14	manganese oxide	ferro		(-0.310+/-0.006)e-3	4.850e-3
15	manganese choride	dia		(-0.251+/-0.005)e-1	1.435e-2
16	nickel-zinc ferrite	para	para	(0.235+/-0.005)e-1	
17	iodized salt	dia		(-7.89+/-0.16)e-5	
18	himalanan salt	dia		(-7.28+/-0.14)e-5	

Table 1: A comparison of our classification and χ_{molar} to what was easily found online. Notice the vast disagreement in the data.

Linearity of Magnetic Field

For these measurements, we assumed that the B-field didn't change considerably over a 2.5 mm displacement from the center of the B_0 . This assumption meant that we just had to measure the change in mass between each step. The error bars on the χ_m 's calculated at each height have been excluded because of how they are skewed from the error in the B_0 calculation. For this reason, all we can conclude is a rough qualitative understanding of the relationship.

It would seem that the internal χ_m is rather linear, for the first 20 or to turns (2.54 mm) After that we seem to get odd behavior where the χ_m seems to return back to zero. What seems to be happening is that we started somewhere below the center line, then shifted above it. As we continued going away once more the impact seemed to reduce back to zero, indicating that we were outside the apex of B_0 .

Discussion and Conclusions

While the general structure of this experiment went well, there must be some discussion on the accuracy of the data. Calibration of B_0 and testing of linearity of χ_m both seemed to work well. The qualitative analysis of diamagnets vs. paramagnets also seemed to follow what was expected to be seen. The χ_m found for most of the materials are off from expected values by nearly a full order of magnitude. This large error is most likely come from human

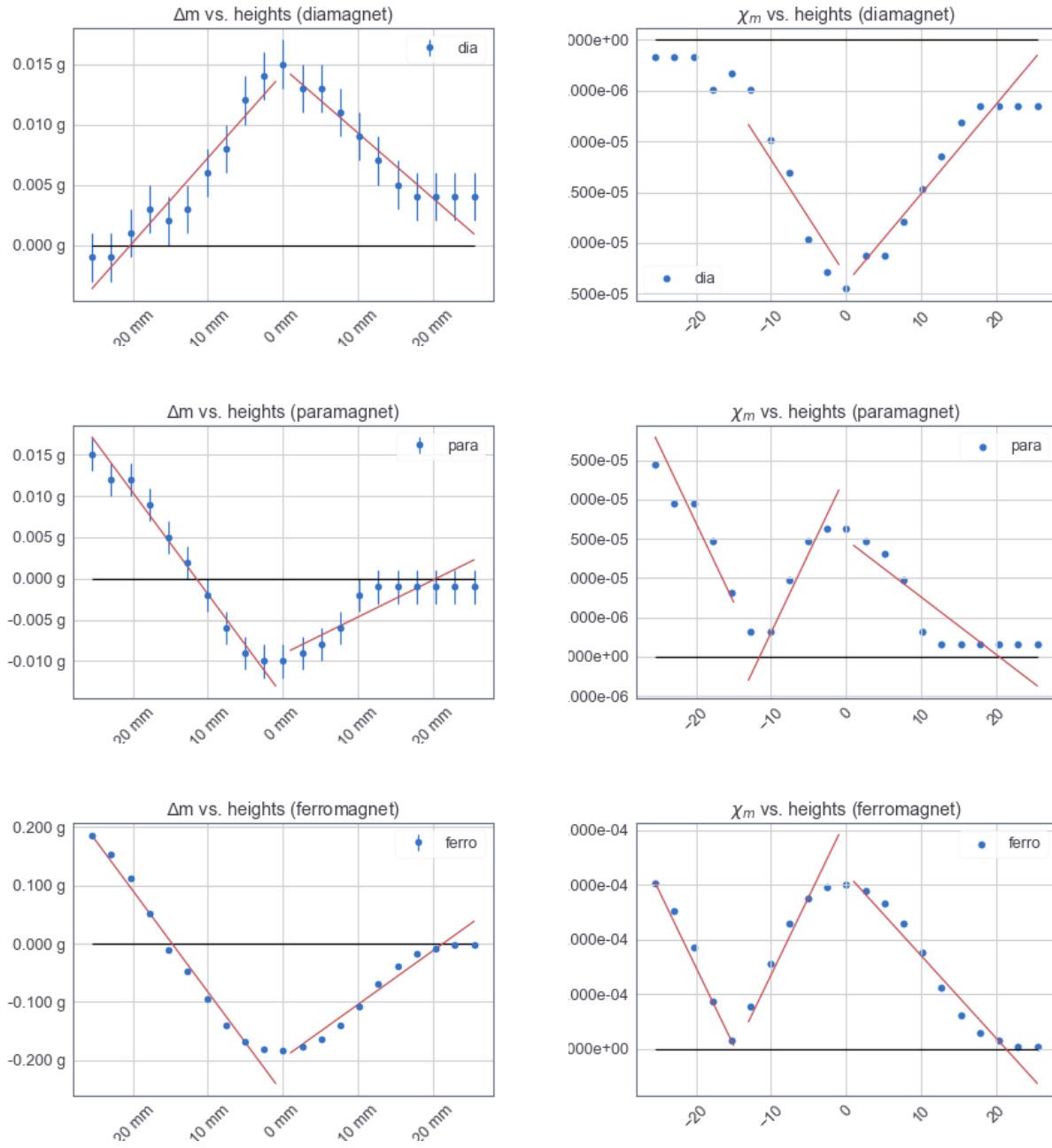


Figure 6: Each plotted Δm and related χ_m at varying heights. The error bars have been removed from the right graphs to allow viewing the trends. Linear fits have been laid atop the graph to help see the linearity of the magnetic susceptibility

error. A lot of data was taken in quick succession, meaning that it is likely that there may have been neglect in where the sample was positioned between the magnets, or not giving enough time for the scale to settle on a value. There is also a chance that the calibration of the scale may have been slightly off, as we had persistent issues both days. We were eventually able to get the accuracy of the measurements within 0.001 g the first day and second days, but that required 3 attempts at calibration. While the data collected may be skewed, the lessons learned were meaningful. If we were given another chance at this lab, it would be worthwhile to work on paying closer attention to the collection of data.

References

- [1] Foundational Magnetic Susceptibility Manual. Teach Spin. Manual provided in lab.
- [2] “Gravity at Bozeman, Mt.” www.wolframalpha.com, Wolfram Alpha LLC, www.wolframalpha.com/input/?i=gravity+at+bozeman%2C+mt. Accessed 3 Oct. 2021.
- [3] Molar Mass Calculator, <https://www.webqc.org/>, 10/03/2021
- [4] Molecular weight and molar mass for chemistry problems, <https://www.convertunits.com/molarmass/>, 10/03/2021
- [5] Themeadow.com. 2021. Minerals in Himalayan Pink Salt: Spectral Analysis — The Meadow. [online] Available at: <https://themeadow.com/pages/minerals-in-himalayan-pink-salt-spectral-analysis>; [Accessed 3 October 2021].
- [6] “Foundational Magnetic Susceptibility.” TeachSpin, www.teachspin.com/fms.

Appendix A

sample	name	mass	height(cm)	volume	molar mass
1	copper	25.22	3.20	3.20	63.55
2	aluminum	7.68	3.00	3.00	26.98
3	titanium	12.95	3.00	3.00	47.87
4	bismuth	18.25	3.30	3.30	208.98
5	colbalt wire	0.26	3.20	0.00	58.93
6	pyrolytic graphite	1.15	3.20	3.20	12.01
7	neodymium choride	4.57	3.10	3.10	358.69
8	gadolinium oxide	6.44	3.40	3.40	362.50
9	erbium oxide	9.31	3.35	3.35	382.52
10	mohrs salt	3.48	3.20	3.20	392.13
11	irom alum	2.11	3.20	3.20	482.25
12	blue vitriol	4.23	3.50	3.50	249.69
13	copper acetate	3.48	3.30	3.30	199.65
14	manganese oxide	5.17	2.90	2.90	70.94
15	manganese choride	3.80	3.50	3.50	925.97
16	nickel-zinc ferrite	5.48	3.40	3.40	234.38
17	empty vial	0.00	3.85	3.85	
1 (redo)	copper	25.22	3.20	3.20	63.55
2 (redo)	aluminum	7.68	3.00	3.00	26.98
3 (redo)	titanium	12.95	3.00	3.00	47.87
4 (redo)	bismuth	18.25	3.30	3.30	208.98
5 (redo)	colbalt wire	0.26	3.20	0.00	58.93
1*	iodized salt	4.81	3.50	3.50	58.44
2*	himalanan salt	4.77	3.70	3.70	58.44
16 (redo)	nickel-zinc ferrite	5.48	3.40	3.40	234.38
5 (second day)	colbalt wire	0.26	3.20	0.00	58.93
2 (second day)	aluminum	7.68	3.00	3.00	26.98
1 (second day)	copper	25.22	3.20	3.20	63.55
18	Rust on paper				

Table 2: Physical statistics of each of the samples. Molar mass data was collected from [3], [4]. More information about the physical description of each can be found in [1]

sample	name	low(g)	high(g)	far(g)	init(g)
1	copper	180.764	180.782	180.772	
2	aluminum	180.779	180.762	180.772	
3	titanium	180.874	180.656	180.772	
4	bismuth	180.701	180.842	180.772	
5	colbalt wire	180.941	180.579	180.771	
6	pyrolytic graphite	180.705	180.841	180.771	180.772
7	neodymium choride	180.939	180.585	180.772	180.772
8	gadolinium oxide	180.155	180.403	180.768	180.774
9	erbium oxide	180.48	180.465	180.767	180.773
10	mohrs salt	180.035	180.426	180.774	180.773
11	iron alum	180.02	180.495	180.773	180.772
12	blue vitriol	180.839	180.693	180.772	180.77
13	copper acetate	180.804	180.734	180.771	180.771
14	manganese oxide	180.472	180.566	180.77	180.772
15	manganese choride	180.512	180.913	180.772	180.775
16	nickel-zinc ferrite	180.622	180.792	180.772	180.776
17	empty vial	180.771	180.78	180.776	180.775
1 (redo)	copper	180.764	180.784	180.775	180.774
2 (redo)	aluminum	180.781	180.764	180.774	180.774
3 (redo)	titanium	180.877	180.655	180.774	180.775
4 (redo)	bismuth	180.705	180.844	180.775	180.774
5 (redo)	colbalt wire	180.943	180.586	180.766	180.766
1*	iodized salt	180.746	180.769	180.759	180.759
2*	himalanan salt	180.748	180.768	180.758	180.758
16 (redo)	nickel-zinc ferrite	181.692	179.777	180.762	180.772
5 (second day)	colbalt wire	180.757	180.58	180.939	180.762
2 (second day)	aluminum	180.762	180.753	180.771	180.763
1 (second day)	copper	180.76	180.77	180.749	180.76
18	Rust on paper	180.763	180.763	180.759	180.76

Table 3: Measured data of the impact on the weight read on the scale each had.